Neurosci. Bull. August, 2019, 35(4):613–623
https://doi.org/10.1007/s12264-019-00377-6

www.neurosci.cn
www.springer.com/12264

ORIGINAL ARTICLE

Increased CXCL13 and CXCR5 in Anterior Cingulate Cortex Contributes to Neuropathic Pain-Related Conditioned Place Aversion

Xiao-Bo Wu[1] · Li-Na He[1] · Bao-Chun Jiang[1] · Xue Wang[1] · Ying Lu[2] · Yong-Jing Gao[1,3]

Received: 7 August 2018 / Accepted: 24 December 2018 / Published online: 30 April 2019

Abstract Pain consists of sensory-discriminative and emotional-affective components. The anterior cingulate cortex (ACC) is a critical brain area in mediating the affective pain. However, the molecular mechanisms involved remain largely unknown. Our recent study indicated that C-X-C motif chemokine 13 (CXCL13) and its sole receptor CXCR5 are involved in sensory sensitization in the spinal cord after spinal nerve ligation (SNL). Whether CXCL13/CXCR5 signaling in the ACC contributes to the pathogenesis of pain-related aversion remains unknown. Here, we showed that SNL increased the CXCL13 level and CXCR5 expression in the ACC after SNL. Knockdown of CXCR5 by microinjection of *Cxcr5* shRNA into the ACC did not affect SNL-induced mechanical allodynia but effectively alleviated neuropathic pain-related place avoidance behavior. Furthermore, electrophysiological recording from layer II–III neurons in the ACC showed that SNL increased the frequency and amplitude of spontaneous excitatory postsynaptic currents (sEPSCs), decreased the EPSC paired-pulse ratio, and increased the α-amino-3-hydroxy-5-methyl-4-isoxazolepropionic acid receptor/N-methyl-D-aspartate receptor ratio, indicating enhanced glutamatergic synaptic transmission. Finally, superfusion of CXCL13 onto ACC slices increased the frequency and amplitude of spontaneous EPSCs. Pre-injection of *Cxcr5* shRNA into the ACC reduced the increase in glutamatergic synaptic transmission induced by SNL. Collectively, these results suggest that CXCL13/CXCR5 signaling in the ACC is involved in neuropathic pain-related aversion *via* synaptic potentiation.

Keywords CXCL13 · CXCR5 · Anterior cingulate cortex · Neuropathic pain · Conditioned place aversion · Synaptic transmission

Introduction

Pain is a complex experience composed of both sensory and affective components. Neuropathic pain caused by peripheral nerve injury is a systemic disease that lacks effective treatment. Clinical observations have shown that patients with neuropathic pain suffer from both severe pain and negative affect such as unpleasantness, aversion, depression, and anxiety [1]. However, the neural and molecular mechanisms of the affective component of neuropathic pain are still unclear.

Although the neuronal pathways and brain areas involved in the affective component of pain remain elusive, accumulating evidence has implicated the anterior cingulate cortex (ACC) as a critical brain region for the emotional processing of pain [2–6]. Neuroimaging studies indicate that ACC activity increases during the presentation of a noxious stimulus and during chronic pain conditions [7, 8]. In animals, lesioning of the ACC abolishes formalin-induced conditioned place avoidance (pain-related aversion) without affecting formalin-induced spontaneous pain behavior (pain sensation) [3, 6, 9]. Microinjection of an

Xiao-Bo Wu and Li-Na He contributed equally to this work.

✉ Yong-Jing Gao
gaoyongjing@ntu.edu.cn; gaoyongjing@hotmail.com

[1] Institute of Pain Medicine, Institute of Special Environmental Medicine, Nantong University, Nantong 226019, China

[2] Department of Nutrition and Food Hygiene, School of Public Health, Nantong University, Nantong 226019, China

[3] Co-innovation Center of Neuroregeneration, Nantong University, Nantong 226001, China

excitatory amino-acid into the ACC produces avoidance learning in the absence of a peripheral noxious stimulus [10]. A recent study has shown that ketamine reduces the aversive response to noxious stimuli in rats with neuropathic pain or inflammatory pain *via* the suppression of neuronal hyperactivity in the ACC [11]. These reports suggest that the ACC is involved in the affective component of pain, but little is known about the molecular mechanisms.

C-X-C motif chemokine 13 (CXCL13), a member of the chemokine family (also known as B lymphocyte chemoattractant) is critical for B-cell recruitment and the functional organization of peripheral lymphoid tissue [12]. CXCL13 is also produced in actively demyelinating multiple sclerosis lesions, and is expressed in perivascular infiltrates and scattered infiltrating cells in lesion parenchyma [13, 14]. CXCR5, the receptor for CXCL13, occurs on all B cells and a subset of T cells in blood, lymphatic tissue, and cerebrospinal fluid [13, 15]. Recent studies have demonstrated that CXCL13 and CXCR5 are expressed in the dorsal root ganglia (DRG), trigeminal ganglion (TG), and spinal cord, and are upregulated under chronic pain conditions [16–18]. For example, the expression of CXCL13 and CXCR5 is increased in neurons of the DRG after complete Freund's adjuvant-induced inflammatory pain [16], and in neurons of the TG after partial infraorbital nerve ligation-induced trigeminal neuropathic pain [17]. CXCL13 is expressed in neurons and CXCR5 in astrocytes in the spinal cord after spinal nerve ligation (SNL) [18]. Also, inhibition of CXCL13/CXCR5 signaling effectively attenuates the pain hypersensitivity induced by inflammation or nerve injury [16, 17, 19].

Accumulating evidence based on animal models of chronic pain has indicated that maladaptive synaptic plasticity in ACC neurons is crucial for pain-related negative emotion [19–21]. Notably, some molecules, such as adenylyl cyclase 1 and the enzyme protein kinase M zeta, are involved in the glutamatergic synaptic plasticity in different layers of the ACC under chronic pain conditions [19, 22, 23]. However, less is known about the effect of CXCL13/CXCR5 on the excitatory synaptic transmission in the ACC under neuropathic pain conditions. In this study, we examined the role of CXCL13/CXCR5 in the ACC in SNL-induced neuropathic pain and negative emotion. We also checked the role of CXCR5 in the glutamatergic transmission of layers II–III neurons of the ACC. Our data suggest that CXCL13/CXCR5 signaling in the ACC contributes to pain-related aversion by regulating the synaptic transmission of ACC pyramidal neurons.

Materials and Methods

Animals and Surgery

Adult ICR mice (male, 6 weeks–8 weeks old) were housed under a 12:12 light–dark cycle with free access to food and water. The animal procedures were reviewed and approved by the Animal Care and Use Committee of Nantong University. All experiments were performed in accordance with the guidelines of the International Association for the Study of Pain. SNL was performed as previously described [18]. In brief, mice were anesthetized with isoflurane and the L6 transverse process was removed to expose the L4 and L5 spinal nerves. The L5 spinal nerve was then isolated and tightly ligated with 6–0 silk. In the sham operation, the L5 spinal nerve was isolated but not ligated.

Real-Time Quantitative PCR (qPCR)

The bilateral ACC was dissected from mice after perfusion with phosphate-buffered saline (PBS). Total RNA extraction, reverse transcription, and qPCR analysis were performed as previously described [25]. The following primers were used: *Cxcl13* forward, 5′-GGC CAC GGT ATT CTG GAA GC-3′; *Cxcl13* reverse, 5′-ACC GAC AAC AGT TGA AAT CAC TC-3′; *Cxcr5* forward, 5′-TGG CCT TCT ACA GTA ACA GCA-3′; *Cxcr5* reverse, 5′-GCA TGA ATA CCG CCT TAA AGG AC-3′; *Gapdh* forward, 5′-AAA TGG TGA AGG TCG GTG TGA AC-3′; *Gapdh* reverse, 5′-CAA CAA TCT CCA CTT TGC CAC TG-3′. The PCR amplification are performed at 95 °C for 30 s, followed by 40 cycles of cycling at 95 °C for 5 s and 60 °C for 45 s. Melting curves were generated to confirm the specificity of the products. Quantification was conducted by normalizing cycle threshold (Ct) values with GAPDH Ct and analyzed with the $2^{-\Delta\Delta CT}$ method.

Elisa

Animals were transcardially perfused with PBS, and the bilateral ACC was dissected. The tissue was homogenized in lysis buffer (Sigma, St. Louis, MO, USA). After determination of the protein concentration by BCA protein assay, 30-μg protein samples were used for assessment of the CXCL13 level according to the manufacturer's protocol (R&D Systems, Minneapolis, MN, USA).

Western Blot

ACC tissue was harvested after perfusion with PBS. Thirty-microgram protein samples were loaded onto SDS–PAGE gel. The separated proteins were then

transferred to PVDF membranes and blocked with 5% milk for 1 h. The following antibodies were added and incubated overnight at 4 °C: CXCR5 (1:100, rabbit, Santa Cruz Dallas, TX, USA) and GAPDH (1:20000, mouse, Millipore, Billerica, MA, USA). After washing with PBS, the membranes were incubated with an HRP-conjugated secondary antibody, developed in enhanced chemiluminescence solution, and exposed on Hyperfilm (Millipore, Billerica, MA). The intensity of selected bands was analyzed using ImageJ software (NIH, Bethesda, MD, USA).

Immunohistochemistry

Immunohistochemistry was performed as described previously [25]. In brief, animals were transcardially perfused with PBS followed by 4% paraformaldehyde. The ACC-containing tissue was removed and postfixed overnight. ACC sections (30 μm, free-floating) were cut on a cryostat. For immunofluorescence, the sections were first blocked with 5% donkey serum for 2 h, followed by CXCR5 antibody (1:100, rabbit, Santa Cruz, Dallas, TX) and NeuN antibody (1:800, mouse, Millipore, Billerica, MA) overnight at 4 °C, and Cy3- or FITC-conjugated secondary antibodies (1:1000, Jackson, West Grove, PA, USA) for 2 h. After that, the sections were examined under a Leica SP8 Gated stimulated emission depletion (STED) confocal microscope.

Fluorescence *In Situ* Hybridization (ISH) and Immunofluorescence Double Staining

The distribution of *Cxcl13* was checked using a *Cxcl13* mRNA ISH Assay Kit (Boster, China) as described previously [18]. The ACC sections (14 μm) were fixed in 4% paraformaldehyde/0.1 mol/L PBS for 30 min and treated with a mixture of 30% H_2O_2 and methanol (v/v, 1:50) for 30 min. The sections were then treated with proteinase K for 2 min at room temperature. After prehybridization, the sections were incubated with a probe specific to *Cxcl13* at 42 °C overnight in hybridization buffer, followed by incubation with mouse-anti-digoxigenin-biotin for 60 min, and SABC-FITC regent (Boster, China) for 30 min.

To identify the neuronal distribution of CXCL13, we incubated the sections with primary antibody against NeuN (1:1000, mouse, Millipore, Billerica, MA) overnight at 4 °C. The Cy3-conjugated secondary antibody was then added and incubated for 2 h. The signal was detected with the Leica SP8 Gated STED confocal microscope.

Lentiviral Vectors Production and Intra-ACC Injection

An shRNA targeting the sequence of *Cxcr5* was designed. The recombinant lentivirus shRNA expressing vectors containing *Cxcr5* shRNA (LV-*Cxcr5* shRNA, 5′-CCA TCA CCT TGT GTG AAT T-3′) or non-specific control (NC) shRNA (LV-NC, 5′-TTC TCC GAA CGT GTC ACG T-3′) were constructed by Shanghai GeneChem using the pGCSIL-GFP vector. The knockdown effect of the LV-*Cxcr5* shRNA was checked *in vitro* using 293FT cells [18].

For lentivirus injection, mice were anesthetized with isoflurane, the head was fixed in a stereotaxic apparatus, and two small holes were drilled on each side (anteroposterior, 1.53 mm; lateral, 0.5 mm). A 32 G syringe was directly lowered into the ACC (depth, 2.0 mm) and 0.3 μl lentivirus solution was injected over a period of 6 min. Before and after injection, the syringe remained in the ACC for 10 min. This procedure was then repeated in the opposite side. The scalp was then sutured.

Behavioral Testing

Animals were habituated to the testing environment daily for 2 days–3 days before experiments. The experimenters were blinded to the treatment.

Von Frey test. Before testing, mice were acclimated for 30 min–60 min on an elevated wire mesh floor. The plantar surface of the left hindpaw was stimulated with a series of von Frey hairs of logarithmically incrementing stiffness (0.02 g–2.56 g, Stoelting, Wood Dale, IL, USA). The 50% paw withdrawal threshold (PWT) was determined using Dixon's up-down method [24]

Conditioned place avoidance (CPA) test. The CPA test was conducted as previously described [26]. Briefly, two 15 cm × 15 cm × 15 cm Plexiglas chambers were placed parallel on top of a mesh screen, and a square door (10 cm per side) was situated between the chambers. One chamber with an opaque ceiling was painted black as a dark area, and the other with a transparent ceiling was painted white as a light area. Before SNL (baseline) and 3 days after SNL, the animals were put into one chamber and allowed free access to the two chambers through the door for 30 min. During this period, a mechanical stimulus (0.16 g) was applied at 15-s intervals to the left paw when the animal was in the dark chamber and to the right paw when the animal was in the light chamber. The time spent in each chamber was recorded every 5 min. The percentage of time spent in the light chamber was calculated for every 5 min and for a total of 30 min. The sham control animals were stimulated and calculations were made in the same way.

Brain Slice Preparation

Coronal brain slices through the ACC were prepared as previously reported [20]. Briefly, mice were anesthetized with isoflurane and decapitated. The brain was rapidly removed and placed in ice-cold oxygenated (95% O_2 + 5% CO_2) artificial cerebrospinal fluid (ACSF) containing (in mmol/L) 230 sucrose, 2.5 KCl, 2.4 $CaCl_2$, 1.2 $MgCl_2$, 11 D-glucose, 1.25 NaH_2PO_4, and 26 $NaHCO_3$. Coronal slices (300 μm) containing the ACC were cut on a vibratome (VT1000 S, Leica Microsystems, Buffalo Grove, IL). The slices were kept in a standard oxygenated ACSF containing (in mmol/L) 125 NaCl, 2.5 KCl, 1.25 NaH_2PO_4, 25 $NaHCO_3$, 11 glucose, 1.2 $MgCl_2$, and 2.4 $CaCl_2$ at 34 °C for 30 min and then at room temperature for at least 1 h before recording.

Whole-Cell Patch-Clamp Recordings

Whole-cell patch clamp was performed under a microscope (BX51WI, Olympus, Tokyo, Japan) equipped with infrared differential interference contrast optics. Brain slices were superfused (2 ml/min–3 ml/min) with oxygenated ACSF at room temperature. The micropipettes were pulled on a P-97 puller (Sutter Instruments, Novato, CA, USA) and had resistances of 3 MΩ–5 MΩ when filled with internal solution containing (in mmol/L) 130 Cs-methanesulfonate, 10 HEPES, 10 CsCl, 4 NaCl, 1 $MgCl_2$, 0.5 EGTA, 5 tetraethylammonium-Cl, 5 MgATP, 0.5 Na_2GTP, and 2.5 QX314 (adjusted to pH 7.2 with CsOH, 290 mOsm). Whole-cell patch clamp recordings were obtained from layer II/III pyramidal neurons in the ACC with a MultiClamp 700B amplifier (Molecular Devices, San Jose, CA, USA). Data were digitized at 10 kHz and filtered at 2 kHz. A seal resistance > 2 GΩ and an access resistance < 35 MΩ were considered acceptable. The cell capacity transients were canceled by the capacitive cancelation circuitry of the amplifier. If the series resistance changed by $> 25\%$ during a recording was excluded from analysis. The $GABA_A$ receptor antagonist picrotoxin (100 μmol/L) was always present in the experiments. After establishing the whole-cell configuration, the membrane potential was held at -70 mV for recording sEPSCs (spontaneous excitatory post-synaptic currents). Cells that showed $> 10\%$ changes from the baseline levels were regarded as responding to the presence of drugs. Evoked EPSCs were generated by a bipolar stimulation electrode with pulses (0.1 Hz) from a stimulation isolation unit controlled by an AMPI generator (Master-8, A.M.P.I., Jerusalem, Israel. The stimulus-evoked currents at -70 mV were identified as α-amino-3-hydroxy-5-methyl-4-isoxazolepropionic acid receptor (AMPAR)-mediated currents. Cells were then held at $+40$ mV, and the amplitude of the evoked EPSCs at 50 ms after the stimulus were considered to be N-methyl-D-aspartate (NMDAR)-mediated currents [27].

Quantification and Statistics

All data are expressed as the mean ± SEM. For Western blots, the density of specific bands was measured with Image J (NIH, Bethesda, MD). The levels of CXCR5 were normalized to GAPDH (loading control). For the quantification of immunoreactive signals, three non-adjacent sections from the ACC were randomly selected. The numbers of CXCL13-, CXCR5-, and NeuN-labeled cells were counted in layers II and III of the ACC in the optic field. The behavioral data were analyzed by two-way repeated-measures ANOVA, and Bonferroni's test was used for *post hoc* multiple-comparison analysis. Differences between two groups were compared using Student's *t*-test. The criterion for statistical significance was $P < 0.05$.

Results

CXCL13 Increases in the ACC After SNL

To examine the CXCL13 expression in the ACC, we first performed quantitative real-time PCR. As shown in Fig. 1A, *Cxcl13* mRNA expression was significantly increased at 1 day (2.1-fold relative to naïve mice, $P < 0.01$), 3 days (5.2-fold, $P < 0.05$), and 10 days (10.8-fold, $P < 0.001$) in SNL-operated mice (SNL *versus* sham, Student's *t*-test), but was not changed in sham-operated animals ($P > 0.05$, one-way ANOVA). ELISA showed a marked increase of CXCL13 protein in the ACC at 1 day (1.7-fold, $P < 0.01$), 3 days (1.4-fold, $P < 0.01$), and 10 days (1.9-fold, $P < 0.001$) after SNL (one-way ANOVA followed by Bonferroni's test, Fig. 1B). We then checked if CXCL13 was produced by neurons. *In situ* hybridization combined with immunostaining showed that 91 ± 4% of $Cxcl13^+$ cells were $NeuN^+$ in layers II–III of the ACC, suggesting the expression of *Cxcl13* in neurons of the ACC (Fig. 1C–E).

CXCR5 Increases in the ACC After SNL

Since CXCR5 is the sole receptor for the chemokine CXCL13 [13], we further examined the expression and distribution of CXCR5 in the ACC after SNL. qPCR showed that CXCR5 mRNA was increased at 3 days (2.8-fold relative to naïve mice) and was maintained at 10 days (2.9-fold, $P < 0.001$ *vs* sham, Student's *t*-test, Fig. 2A). Western blot further showed an increased protein level of

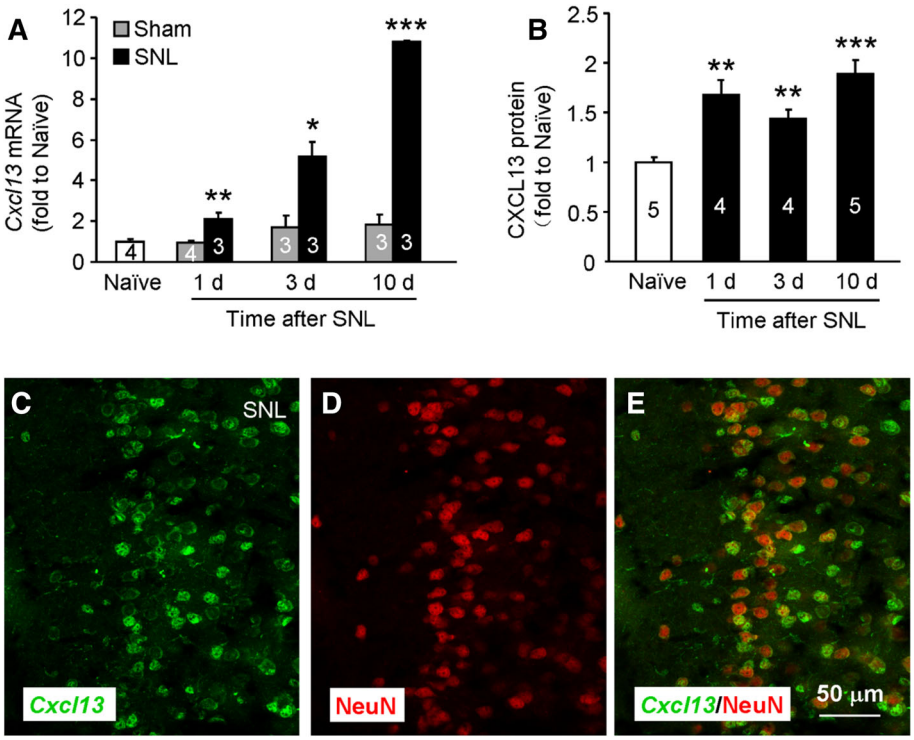

Fig. 1 SNL induces CXCL13 upregulation in the ACC. **A** Real-time PCR results showing an increase of *Cxcl13* mRNA expression in the ACC. *Cxcl13* mRNA expression gradually increased from 1 to 10 days after SNL (*$P < 0.05$, **$P < 0.01$, ***$P < 0.001$ *vs* sham. **B** ELISA showing that CXCL13 protein expression was increased in the ACC at 1, 3, and 10 days (**$P < 0.01$, ***$P < 0.001$ *vs* naïve mice. **C–E** *In situ* hybridization of *Cxcl13* (**C**) combined with immunostaining of NeuN (**D**) showing that CXCL13 was co-localized with the neuronal marker NeuN (**E**).

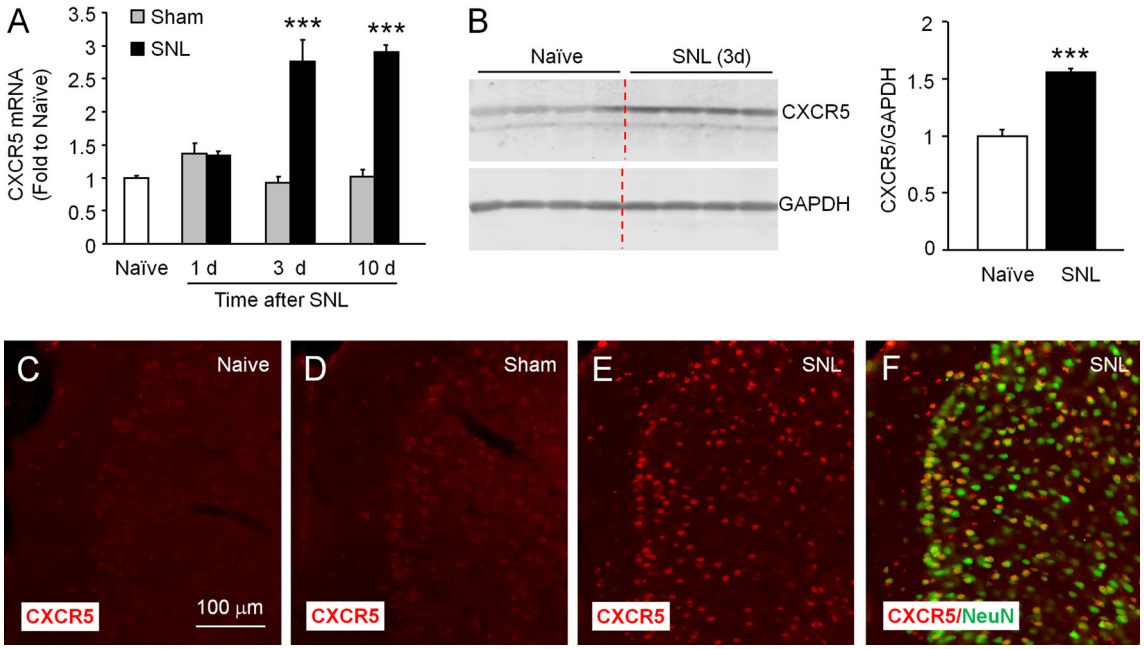

Fig. 2 SNL increases CXCR5 expression in the ACC. **A** Real-time PCR results showing an increase of *Cxcr5* mRNA expression in the ACC. *Cxcr5* mRNA was increased at 3 and 10 days after SNL (***$P < 0.001$ *vs* sham). **B** Western blots showing that CXCR5 protein expression was markedly increased in the ACC after SNL ($n = 4$ mice/group). **C–E** Immunostaining showing CXCR5 expression in the ACC in naïve (**C**), sham (**D**), and SNL (3 days) (**E**) mice. **F** Double staining showing the co-localization of CXCR5 with the neuronal marker NeuN.

CXCR5 (1.6-fold) 3 days after SNL ($P < 0.001$ *vs* naïve mice, Student's *t*-test, Fig. 2B). Immunostaining showed low expression of CXCR5 in naïve (Fig. 2C) and sham-operated mice (Fig. 2D), but markedly increased expression in SNL mice (Fig. 2E). Double staining for CXCR5 and NeuN showed that 94 ± 3% of CXCR5$^+$ cells were co-localized with NeuN (Fig. 2F) in layers II–III,

indicating the predominant production of CXCR5 by neurons in the ACC.

Knockdown of *Cxcr5* in the ACC Alleviates SNL-induced Pain-Related Aversion

To check the role of CXCR5 in SNL-induced pain hypersensitivity and pain-related aversion, we first assessed the mechanical allodynia and conditioned place avoidance after SNL. As previously reported [28], SNL induced a robust decrease of the PWT of the ipsilateral hindpaw ($P < 0.01$, two-way ANOVA, Fig. 3A). We further assessed the pain-related aversion with the CPA test. As shown in Fig. 3B–C, before sham or SNL operation, the animals spent similar times in the light chamber within the 30 min (Sham, 35.7 ± 4.4%; SNL, 36.8 ± 3.0%, $P > 0.05$, Student's *t*-test). However, three days after operation, while the sham-operated animals spent a similar time (32.6 ± 5.0%) in the light chamber, the SNL-operated animals spent much more time (61.1 ± 6.2%) in the light chamber ($P < 0.001$), suggesting the development of neuropathic pain-related place avoidance in the SNL mice.

We then microinjected LV-*Cxcr5* shRNA or LV-NC into the bilateral ACC 7 days before SNL (Fig. 3D). LV-*Cxcr5* shRNA significantly reduced *Cxcr5* mRNA expression compared to microinjection of LV-NC ($P < 0.05$, Student's *t*-test, Fig. 3E). Behavioral tests showed that, 3 days after SNL, LV-*Cxcr5* shRNA did not affect mechanical allodynia compared to the LV-NC group. However, the pain-related aversion induced by SNL was significantly attenuated in animals injected with LV-*Cxcr5* shRNA, compared with the LV-NC group ($P < 0.05$, Student's *t*-

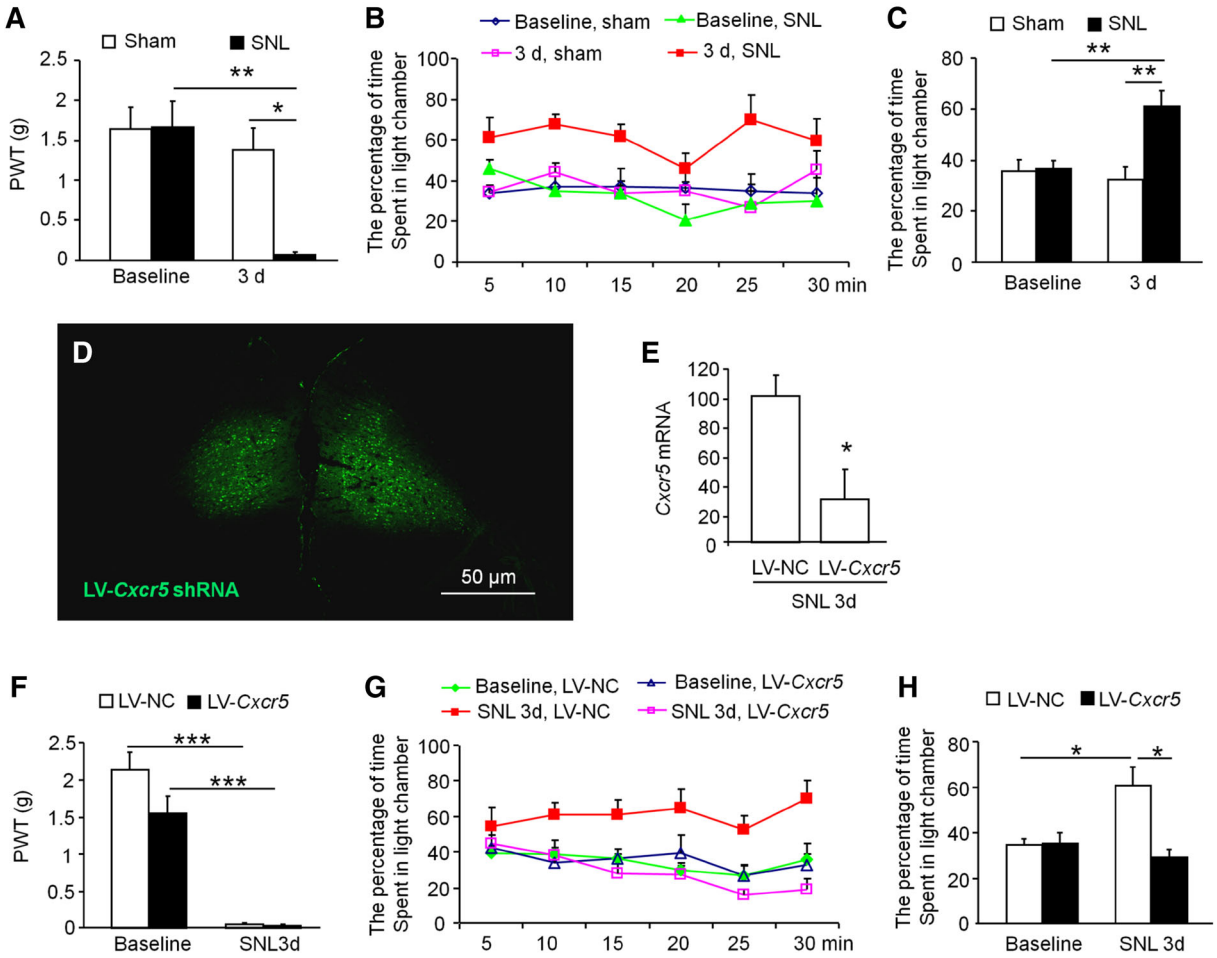

Fig. 3 SNL-related aversion is relieved after CXCR5 knockdown in the ACC. **A** SNL induced mechanical allodynia 3 days after SNL (*$P < 0.05$, **$P < 0.01$, two-way repeated-measures ANOVA followed by Bonferroni's test; $n = 5$ mice/group; PWT, paw withdrawal threshold). **B** Time-course showing that a conditioned place aversion behavior was induced in SNL mice, expressed as the percentage of time for mouse spent in the lighted chamber. **C** Summary of aversion behavior in 30 min (**$P < 0.01$, $n = 5$ mice/group). **D** Expression of GFP in the ACC 7 days after intra-ACC injection. **E** Expression of *Cxcr5* mRNA was markedly decreased in mice with LV-*Cxcr5* shRNA intra-ACC injection 7 days before the SNL operation. **F** Inhibition of CXCR5 by LV-*Cxcr5* shRNA did not affect the SNL-induced mechanical allodynia (***$P < 0.001$; $n = 6$–7 mice/group; PWT, paw withdrawal threshold). **G**, **H** Inhibition of CXCR5 by LV-*Cxcr5* shRNA markedly alleviated the aversive behavior induced by SNL (*$P < 0.05$, $n = 6$–7 mice/group).

test, Fig. 3F–H), suggesting the involvement of CXCR5 in SNL-induced pain aversion.

SNL Enhances Glutamatergic Synaptic Transmission in the ACC

To further determine the mechanisms of CXCL13/CXCR5 underlying pain aversion, we prepared ACC slices and performed whole-cell recording in the pyramidal neurons of layers II–III of the ACC. In SNL mice, both the frequency and amplitude of the sEPSCs were significantly increased at postoperative day 3 compared with sham-operated mice ($P < 0.05$ or < 0.01, Student's *t*-test, Fig. 4A–C). Paired-pulse facilitation is a measure of short-term plasticity that is widely used to test for changes in presynaptic function. As shown in Fig. 4D, the paired-pulse ratio (PPR) was lower in SNL mice than in sham-operated mice, suggesting that SNL causes a change in the probability of transmitter release. To further determine the postsynaptic mechanism, we compared the relative contribution of AMPAR- and NMDAR-mediated currents. As shown in Fig. 4E, the AMPAR/NMDAR ratio was markedly higher at synapses on neurons in SNL mice than in sham-operated mice ($P < 0.05$, Student's *t*-test). These results indicate that the presynaptic glutamate transmitter release and postsynaptic responses in the ACC are enhanced in SNL mice.

CXCL13 and CXCR5 Contribute to the Enhanced Synaptic Transmission After SNL

We then checked whether CXCL13 and CXCR5 in the ACC are involved in the enhanced synaptic transmission after SNL. We first measured the effect of CXCL13 on the basal glutamatergic synaptic transmission. Superfusion with CXCL13 (100 ng/ml) increased the frequency and amplitude of sEPSCs in 5 of 8 neurons recorded from naïve mice ($P < 0.05$ or < 0.01, paired Student's *t*-test, Fig. 5A–C). We then tested the synaptic transmission in pyramidal neurons from SNL mice pre-injected with LV-*Cxcr5* shRNA or LV-NC (Fig. 5D). Both the frequency and amplitude of sEPSCs were markedly lower in SNL mice treated with LV-*Cxcr5* shRNA ($P < 0.05$, Student's *t*-test, Fig. 5E–G). However, the change of PPR induced by SNL was not significantly different in the *Cxcr5*-knockdown mice ($P > 0.05$, Student's *t*-test, Fig. 5H). We further examined the AMPAR/NMDAR ratio and found that knockdown of CXCR5 decreased the AMPAR/NMDAR ratio compared to LV-NC ($P < 0.05$, Student's *t*-test, Fig. 5I). Taken together, our results suggest that CXCL13/CXCR5 in the ACC is involved in pain-related aversion by

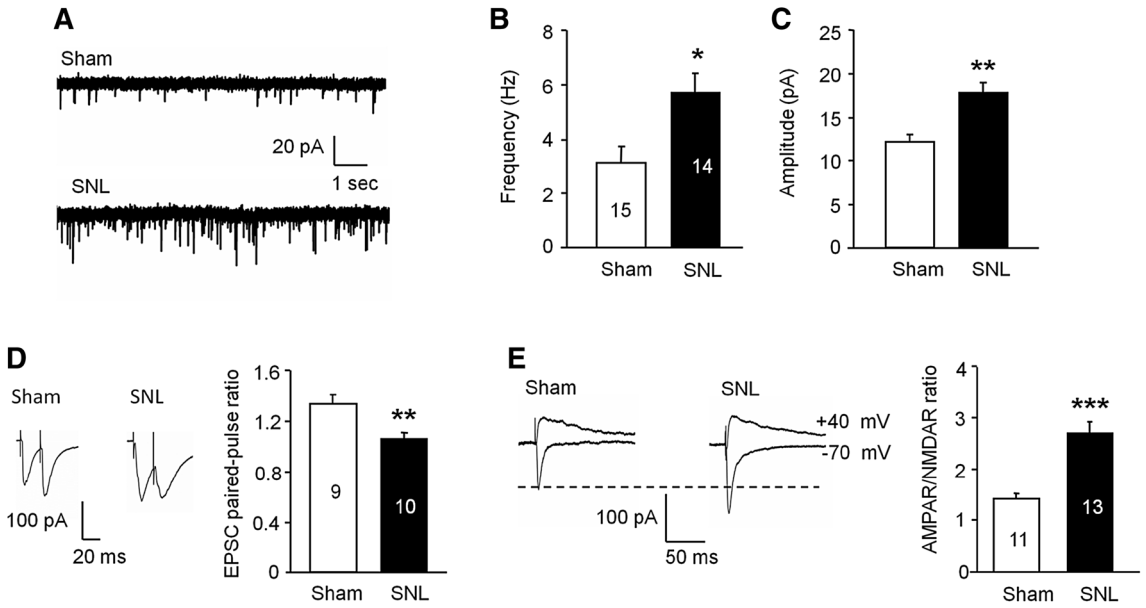

Fig. 4 SNL enhances glutamatergic synaptic transmission in the neurons of layers II–III of the ACC. **A** Representative sEPSCs at ACC synapses in sham-operated and SNL mice at a holding potential of − 70 mV (scale bars, 20 pA and 1 s). **B**, **C** Compared to the sham group, the mean frequency (**B**) and amplitude (**C**) of sEPSCs were increased in the SNL group (*$P < 0.05$, Student's *t*-test; sham, $n = 15$ and 5 mice; SNL, $n = 14$ and 4 mice). **D** Paired-pulse traces of EPSC recordings from sham- and SNL-operated mice (**$P < 0.01$, Student's *t*-test; sham, $n = 9$ and 3 mice; SNL, $n = 10$ and 4 mice). **E** Sample traces showing AMPAR- (downward) and NMDAR- (upward) mediated EPSCs recorded at holding potentials of − 70 mV and + 40 mV, respectively. Summary histograms show the increased AMPAR/NMDAR ratio of ACC neurons in the SNL group compared with sham-operated mice (***$P < 0.001$, Student's *t*-test; sham, $n = 11$ and 4 mice; SNL, $n = 13$ and 5 mice).

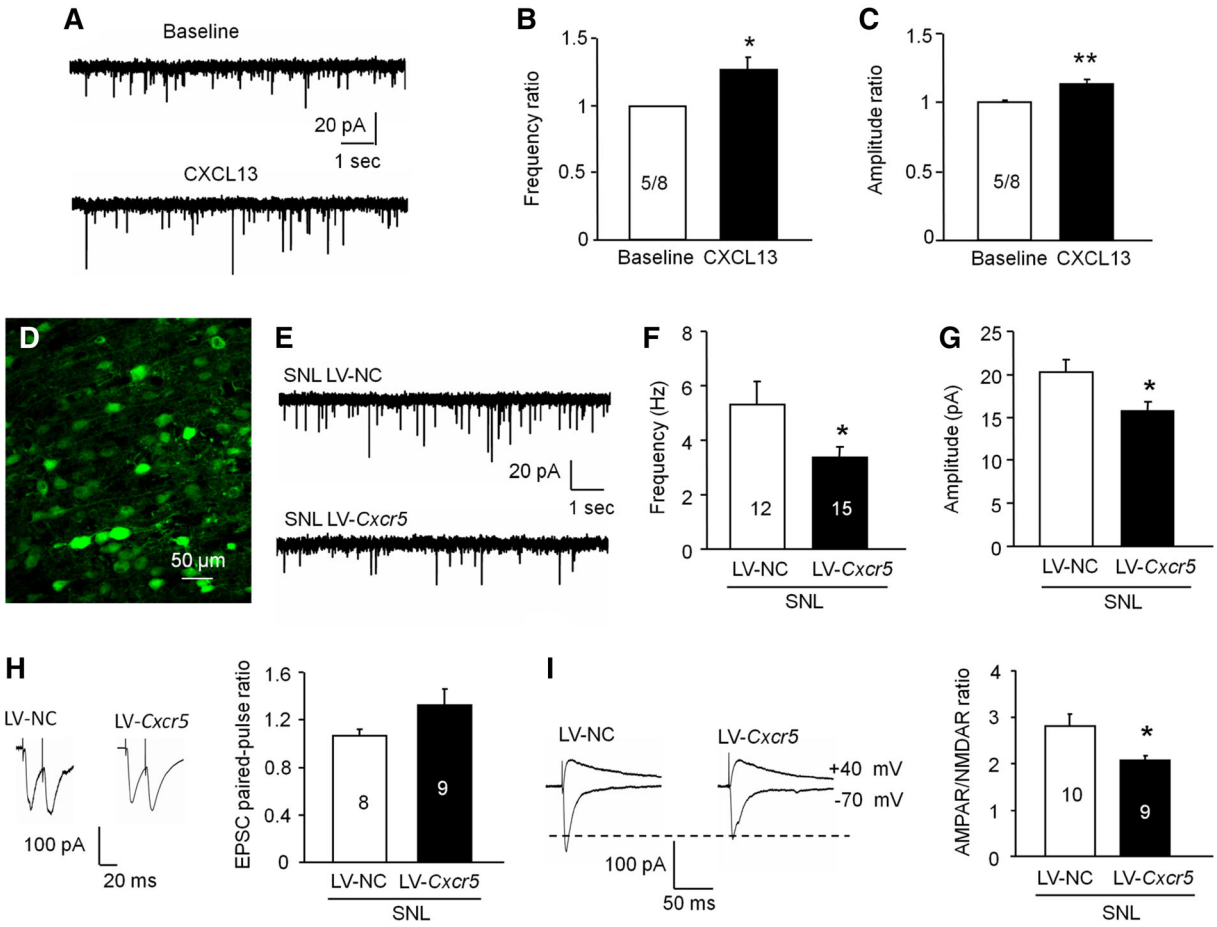

Fig. 5 CXCR5 is involved in the synaptic transmission of pyramidal neurons in layers II/III of the ACC. **A** Sample traces of sEPSCs with or without CXCL13 perfusion. **B**, **C** Frequency (**B**) and amplitude (**C**) of sEPSCs were increased after CXCL13 incubation (5 of 8 neurons, $*P < 0.05$, paired Student's *t*-test). **D** Representative image of intra-ACC injection of LV-*Cxcr5* siRNA. **E** Sample traces of sEPSCs recorded in SNL mice with pre-injection of LV-NC or LV-*Cxcr5* shRNA into the ACC. **F**, **G** Knockdown of *Cxcr5* by shRNA abolished the increased frequency (**F**) and amplitude (**G**) of sEPSCs in SNL mice ($*P < 0.05$, Student's *t*-test; LV-NC, $n = 12$ and 3 mice; LV-*Cxcr5* shRNA, $n = 15$ and 4 mice). **H** Paired-pulse traces of EPSC recordings from sham- and SNL-operated mice (no significant difference). **I** Sample traces of AMPAR and NMDAR currents in mice pre-injected with LV-NC or LV-*Cxcr5* shRNA. Summary histograms showing that LV-*Cxcr5* shRNA abolished the increase in AMPAR/NMDAR ratio ($*P < 0.05$, Student's *t*-test; LV-NC, $n = 10$ and 3 mice; LV-*Cxcr5*, $n = 9$ and 3 mice).

enhancing postsynaptic glutamatergic receptor-mediated excitatory synaptic transmission during neuropathic pain.

Discussion

In this study, we investigated the expression of CXCL13 and CXCR5 in the ACC after SNL and the role of CXCR5 in pain sensation and pain affect. We found that SNL markedly increased the expression of CXCL13 and CXCR5 in the ACC. Knockdown of CXCR5 in the ACC attenuated pain-related conditioned place avoidance, but not mechanical allodynia. Finally, SNL induced synaptic potentiation in the pyramidal neurons of layers II–III, and this was reduced by knockdown of CXCR5. Our data suggest that CXCL13/CXCR5 signaling in the ACC is involved in the pain-related aversive emotion *via* regulating glutamatergic synaptic transmission.

Neuroinflammation mediated by pro-inflammatory cytokines and chemokines is involved in a variety of diseases, including neurodegenerative diseases such as multiple sclerosis and Alzheimer's disease, and neurological disorders such as stroke and trauma [29–31]. Accumulating evidence suggests that chemokines in the spinal cord and DRG play a pivotal role in the development and maintenance of chronic pain [32–34]. However, the expression and role of chemokines in supraspinal areas under chronic pain condition are less studied. It has been reported that CCL2, CCL3, and CCR2 are increased in the hippocampus, CCR1 and CCR2 are increased in the thalamus, and CCL3 is increased in the periaqueductal gray in a neuropathic pain model induced by spinal cord

injury [35]. We report here the upregulation of CXCL13 and CXCR5 in the neurons of ACC layers II–III, although we do not exclude their possible distribution in glial cells. Similarly, CXCL13 and CXCR5 are expressed in neurons in the DRG and TG, co-localized with calcitonin gene-related peptide, isolectin-B4, and neurofilament 200 [16, 17]. However, CXCL13 and CXCR5 are expressed in neurons and astrocytes, respectively, in the spinal cord, and CXCL13 mediates neuropathic pain *via* CXCR5-dependent astrocyte activation [18]. These data suggest that the distribution of the chemokine and its receptor is tissue-specific, and chemokines contribute to different physiological or pathological function *via* different mechanisms.

Previous studies have shown that direct blocking of CXCR5 function in peripheral sensory neurons or the spinal cord attenuates pain hypersensitivity under chronic pain conditions [16–18]. Preclinical study has also shown that chemokines are linked to peripheral-central crosstalk and may contribute to emotional and cognitive disorders. Clinical data analysis has reported that higher levels of CXCL4 and CXCL7 are associated with depression [36]. In an animal model, a recent study reported that activation of $CX3CR1^{+}$ monocytes causes dendritic spine loss on layer V pyramidal neurons in the cortex, and induced cognitive dysfunction [37]. Here we found a negative effect associated with neuropathy-induced hypersensitivity in SNL mice. Previous studies have shown that a lesion in the ACC prevents the negative effect of chronic pain without affecting the tactile mechanical allodynia [9, 38]. In addition, inhibition of SIP30 (SNARE complex SNAP25 interaction protein) in the ACC blocks pain-related aversion and anxiety but does not affect mechanical allodynia and heat hyperalgesia induced by chronic constriction injury of the sciatic nerve [39]. Our results indicated that the aversive but not the sensory components of neuropathic pain was attenuated with shRNA silencing of CXCR5 in the ACC, supporting the role of the ACC in higher-order processing of noxious information [21, 38, 40].

Our study also provides a mechanistic basis for the influence of CXCL13/CXCR5 signaling on pain aversion. Cumulative evidence suggests that persistent peripheral injury triggers presynaptic glutamate release and neuronal hyperexcitability in the ACC [19, 22, 23]. In addition, ACC hyperactivity (shown as increased excitatory postsynaptic transmission) coincides with the time window of pain aversion and of anxiodepressive-like behaviors [41]. Optogenetic inhibition of the ACC is sufficient to counteract the neuropathic pain-induced emotional consequences [41]. Consistent with these studies, we recorded a change of glutamate synaptic transmission in ACC pyramidal neurons in SNL-operated mice. Meanwhile, postsynaptic changes in AMPAR-mediated responses were prevented in SNL-operated mice with shRNA silencing of CXCR5 in the ACC. Although the sEPSC frequency indirectly reflects presynaptic glutamate release, postsynaptic AMPARs might also play a critical role [42, 43]. Reversal of the AMPAR/NMDAR ratio with shRNA silencing of CXCR5 in the ACC was accompanied by decreased AMPAR-mediated EPSC frequency and amplitude, while the PPR was not significantly changed, suggesting that CXCR5-knockdown decreases the number or function of postsynaptic AMPARs rather than alterations of presynaptic glutamate release [44]. Similar effects have also been reported on other chemokine family members, such as CCL2 [45], CXCL10 [46], and CXCL16 [47], which play important roles in the modulation of synaptic transmission in hippocampal neurons in mice. Toyoda *et al*. reported that the AMPAR subunit GluA1 and extracellular signal-regulated kinase (ERK) are involved in long-term potentiation in the ACC [48, 49]. Also, complete Freund's adjuvant-induced ERK activation in the ACC is reduced in $GluA1^{-/-}$ mice [48], suggesting that the GluA1-ERK pathway plays an important role in synaptic plasticity in the ACC. Our previous studies demonstrated that CXCR5 induces ERK activation in the TG and spinal cord [17, 18], and ERK activation in the ACC contributes to the induction and expression of formalin-induced affective pain [4]. Behavioral studies have also shown that inhibition of ERK in the ACC blocks pain-related aversion, but does not affect chronic constriction injury-induced mechanical allodynia and heat hyperalgesia [39]. Thus, CXCL13/CXCR5 signaling may be involved in nerve injury-induced pain aversion *via* AMPAR subunit modulation and ERK activation in the ACC. However, detailed molecular evidence for CXCL13/CXCR5 signaling in synaptic plasticity needs further research.

The ACC is a part of the limbic system, which is known to be engaged in cognitive and emotional processing. Some mental disorders such as anxiety, depression, cognitive impairment, and schizophrenia are associated with maladaptive changes of ACC neuronal activity and synaptic transmission, which may result from disruption of the balance of excitatory and inhibitory connectivity [41, 50, 51]. In addition, inflammation in the ACC may contribute to major depressive episodes [50, 52]. Whether CXCL13 and CXCR5 mediate mood disorders other than pain aversion remains to be investigated.

In summary, our results demonstrated that peripheral nerve injury increased the level of the chemokine CXCL13 and its receptor CXCR5 in the ACC. Knockdown of CXCR5 in the ACC by shRNA silencing alleviated the negative affective component of neuropathic pain, possibly mediated by the regulation of synaptic transmission in ACC pyramidal neurons. Targeting CXCL13/CXCR5 signaling in the ACC may be an effective strategy for the treatment of neuropathic pain-related negative effect.

Acknowledgements This work was supported by grants from the National Natural Science Foundation of China (31671091 and 81771197), the Natural Science Foundation of Jiangsu Province, China (BK20171255), and the Science and Technology Planning Project of Nantong Municipality, China (MS12017023-9).

References

1. Miller LR, Cano A. Comorbid chronic pain and depression: who is at risk? J Pain 2009, 10: 619–627.
2. LaGraize SC, Borzan J, Peng YB, Fuchs PN. Selective regulation of pain affect following activation of the opioid anterior cingulate cortex system. Exp Neurol 2006, 197: 22–30.
3. Gao YJ, Ren WH, Zhang YQ, Zhao ZQ. Contributions of the anterior cingulate cortex and amygdala to pain- and fear-conditioned place avoidance in rats. Pain 2004, 110: 343–353.
4. Cao H, Gao YJ, Ren WH, Li TT, Duan KZ, Cui YH, *et al.* Activation of extracellular signal-regulated kinase in the anterior cingulate cortex contributes to the induction and expression of affective pain. J Neurosci 2009, 29: 3307–3321.
5. Qu C, King T, Okun A, Lai J, Fields HL, Porreca F. Lesion of the rostral anterior cingulate cortex eliminates the aversiveness of spontaneous neuropathic pain following partial or complete axotomy. Pain 2011, 152: 1641–1648.
6. Johansen JP, Fields HL, Manning BH. The affective component of pain in rodents: direct evidence for a contribution of the anterior cingulate cortex. Proc Natl Acad Sci USA 2001, 98: 8077–8082.
7. Cifre I, Sitges C, Fraiman D, Munoz MA, Balenzuela P, Gonzalez-Roldan A, *et al.* Disrupted functional connectivity of the pain network in fibromyalgia. Psychosom Med 2012, 74: 55–62.
8. Yuan W, Dan L, Netra R, Shaohui M, Chenwang J, Ming Z. A pharmaco-fMRI study on pain networks induced by electrical stimulation after sumatriptan injection. Exp Brain Res 2013, 226: 15–24.
9. LaGraize SC, Labuda CJ, Rutledge MA, Jackson RL, Fuchs PN. Differential effect of anterior cingulate cortex lesion on mechanical hypersensitivity and escape/avoidance behavior in an animal model of neuropathic pain. Exp Neurol 2004, 188: 139–148.
10. Johansen JP, Fields HL. Glutamatergic activation of anterior cingulate cortex produces an aversive teaching signal. Nat Neurosci 2004, 7: 398–403.
11. Zhou H, Zhang Q, Martinez E, Dale J, Hu S, Zhang E, *et al.* Ketamine reduces aversion in rodent pain models by suppressing hyperactivity of the anterior cingulate cortex. Nat Commun 2018, 9: 3751.
12. Ansel KM, Ngo VN, Hyman PL, Luther SA, Forster R, Sedgwick JD, *et al.* A chemokine-driven positive feedback loop organizes lymphoid follicles. Nature 2000, 406: 309–314.
13. Krumbholz M, Theil D, Cepok S, Hemmer B, Kivisakk P, Ransohoff RM, *et al.* Chemokines in multiple sclerosis: CXCL12 and CXCL13 up-regulation is differentially linked to CNS immune cell recruitment. Brain 2006, 129: 200–211.
14. Rainey-Barger EK, Rumble JM, Lalor SJ, Esen N, Segal BM, Irani DN. The lymphoid chemokine, CXCL13, is dispensable for the initial recruitment of B cells to the acutely inflamed central nervous system. Brain Behav Immun 2011, 25: 922–931.
15. Kim CH, Rott LS, Clark-Lewis I, Campbell DJ, Wu L, Butcher EC. Subspecialization of CXCR5+ T cells: B helper activity is focused in a germinal center-localized subset of CXCR5+ T cells. J Exp Med 2001, 193: 1373–1381.
16. Wu XB, Cao DL, Zhang X, Jiang BC, Zhao LX, Qian B, *et al.* CXCL13/CXCR5 enhances sodium channel Nav1.8 current density via p38 MAP kinase in primary sensory neurons following inflammatory pain. Sci Rep 2016, 6: 34836.
17. Zhang Q, Cao DL, Zhang ZJ, Jiang BC, Gao YJ. Chemokine CXCL13 mediates orofacial neuropathic pain via CXCR5/ERK pathway in the trigeminal ganglion of mice. J Neuroinflamm 2016, 13: 183.
18. Jiang BC, Cao DL, Zhang X, Zhang ZJ, He LN, Li CH, *et al.* CXCL13 drives spinal astrocyte activation and neuropathic pain via CXCR5. J Clin Invest 2016, 126: 745–761.
19. Li XY, Ko HG, Chen T, Descalzi G, Koga K, Wang H, *et al.* Alleviating neuropathic pain hypersensitivity by inhibiting PKMzeta in the anterior cingulate cortex. Science 2010, 330: 1400–1404.
20. Wu LJ, Toyoda H, Zhao MG, Lee YS, Tang J, Ko SW, *et al.* Upregulation of forebrain NMDA NR2B receptors contributes to behavioral sensitization after inflammation. J Neurosci 2005, 25: 11107–11116.
21. Koga K, Descalzi G, Chen T, Ko HG, Lu J, Li S, *et al.* Coexistence of two forms of LTP in ACC provides a synaptic mechanism for the interactions between anxiety and chronic pain. Neuron 2015, 85: 377–389.
22. Xu H, Wu LJ, Wang H, Zhang X, Vadakkan KI, Kim SS, *et al.* Presynaptic and postsynaptic amplifications of neuropathic pain in the anterior cingulate cortex. J Neurosci 2008, 28: 7445–7453.
23. Blom SM, Pfister JP, Santello M, Senn W, Nevian T. Nerve injury-induced neuropathic pain causes disinhibition of the anterior cingulate cortex. J Neurosci 2014, 34: 5754–5764.
24. Chaplan SR, Bach FW, Pogrel JW, Chung JM, Yaksh TL. Quantitative assessment of tactile allodynia in the rat paw. J Neurosci Methods 1994, 53: 55–63.
25. Jing PB, Cao DL, Li SS, Zhu M, Bai XQ, Wu XB, *et al.* Chemokine receptor CXCR3 in the spinal cord contributes to chronic itch in mice. Neurosci Bull 2018, 34: 54–63.
26. Chen FL, Dong YL, Zhang ZJ, Cao DL, Xu J, Hui J, *et al.* Activation of astrocytes in the anterior cingulate cortex contributes to the affective component of pain in an inflammatory pain model. Brain Res Bull 2012, 87: 60–66.
27. Du J, Creson TK, Wu LJ, Ren M, Gray NA, Falke C, *et al.* The role of hippocampal GluR1 and GluR2 receptors in manic-like behavior. J Neurosci 2008, 28: 68–79.
28. Zhang ZJ, Cao DL, Zhang X, Ji RR, Gao YJ. Chemokine contribution to neuropathic pain: respective induction of CXCL1 and CXCR2 in spinal cord astrocytes and neurons. Pain 2013, 154: 2185–2197.
29. Mennicken F, Maki R, de Souza EB, Quirion R. Chemokines and chemokine receptors in the CNS: a possible role in neuroinflammation and patterning. Trends Pharmacol Sci 1999, 20: 73–78.
30. Ubogu EE, Cossoy MB, Ransohoff RM. The expression and function of chemokines involved in CNS inflammation. Trends Pharmacol Sci 2006, 27: 48–55.
31. Savarin-Vuaillat C, Ransohoff RM. Chemokines and chemokine receptors in neurological disease: raise, retain, or reduce? Neurotherapeutics 2007, 4: 590–601.
32. Zhang ZJ, Jiang BC, Gao YJ. Chemokines in neuron-glial cell interaction and pathogenesis of neuropathic pain. Cell Mol Life Sci 2017, 74: 3275–3291.
33. Bai L, Wang X, Li Z, Kong C, Zhao Y, Qian JL, *et al.* Upregulation of chemokine CXCL12 in the dorsal root ganglia and spinal cord contributes to the development and maintenance of neuropathic pain following spared nerve injury in rats. Neurosci Bull 2016, 32: 27–40.
34. Xie RG, Gao YJ, Park CK, Lu N, Luo C, Wang WT, *et al.* Spinal CCL2 promotes central sensitization, long-term potentiation, and inflammatory pain via CCR2: further insights into molecular, synaptic, and cellular mechanisms. Neurosci Bull 2018, 34: 13–21.

35. Knerlich-Lukoschus F, Noack M, von der Ropp-Brenner B, Lucius R, Mehdorn HM, Held-Feindt J. Spinal cord injuries induce changes in CB1 cannabinoid receptor and C-C chemokine expression in brain areas underlying circuitry of chronic pain conditions. J Neurotrauma 2011, 28: 619–634.
36. Leighton SP, Nerurkar L, Krishnadas R, Johnman C, Graham GJ, Cavanagh J. Chemokines in depression in health and in inflammatory illness: a systematic review and meta-analysis. Mol Psychiatry 2017, 23:48–58.
37. Garre JM, Silva HM, Lafaille JJ, Yang G. CX3CR1+ monocytes modulate learning and learning-dependent dendritic spine remodeling via TNF-alpha. Nat Med 2017, 23: 714–722.
38. Barthas F, Sellmeijer J, Hugel S, Waltisperger E, Barrot M, Yalcin I. The anterior cingulate cortex is a critical hub for pain-induced depression. Biol Psychiatry 2015, 77: 236–245.
39. Han M, Xiao X, Yang Y, Huang RY, Cao H, Zhao ZQ, *et al.* SIP30 is required for neuropathic pain-evoked aversion in rats. J Neurosci 2014, 34: 346–355.
40. Zhang Q, Manders T, Tong AP, Yang R, Garg A, Martinez E, *et al.* Chronic pain induces generalized enhancement of aversion. Elife 2017, 6.
41. Sellmeijer J, Mathis V, Hugel S, Li XH, Song Q, Chen QY, *et al.* Hyperactivity of anterior cingulate cortex areas 24a/24b drives chronic pain-induced anxiodepressive-like consequences. J Neurosci 2018, 38: 3102–3115.
42. Anggono V, Huganir RL. Regulation of AMPA receptor trafficking and synaptic plasticity. Curr Opin Neurobiol 2012, 22: 461–469.
43. Kavalali ET. The mechanisms and functions of spontaneous neurotransmitter release. Nat Rev Neurosci 2015, 16: 5–16.
44. Argilli E, Sibley DR, Malenka RC, England PM, Bonci A. Mechanism and time course of cocaine-induced long-term potentiation in the ventral tegmental area. J Neurosci 2008, 28: 9092–9100.
45. Zhou Y, Tang H, Liu J, Dong J, Xiong H. Chemokine CCL2 modulation of neuronal excitability and synaptic transmission in rat hippocampal slices. J Neurochem 2011, 116: 406–414.
46. Vlkolinsky R, Siggins GR, Campbell IL, Krucker T. Acute exposure to CXC chemokine ligand 10, but not its chronic astroglial production, alters synaptic plasticity in mouse hippocampal slices. J Neuroimmunol 2004, 150: 37–47.
47. Di Castro MA, Trettel F, Milior G, Maggi L, Ragozzino D, Limatola C. The chemokine CXCL16 modulates neurotransmitter release in hippocampal CA1 area. Sci Rep 2016, 6: 34633.
48. Toyoda H, Zhao MG, Ulzhofer B, Wu LJ, Xu H, Seeburg PH, *et al.* Roles of the AMPA receptor subunit GluA1 but not GluA2 in synaptic potentiation and activation of ERK in the anterior cingulate cortex. Mol Pain 2009, 5: 46.
49. Toyoda H, Zhao MG, Xu H, Wu LJ, Ren M, Zhuo M. Requirement of extracellular signal-regulated kinase/mitogen-activated protein kinase for long-term potentiation in adult mouse anterior cingulate cortex. Mol Pain 2007, 3: 36.
50. Holmes SE, Hinz R, Conen S, Gregory CJ, Matthews JC, Anton-Rodriguez JM, *et al.* Elevated translocator protein in anterior cingulate in major depression and a role for inflammation in suicidal thinking: a positron emission tomography study. Biol Psychiatry 2018, 83: 61–69.
51. Shukla DK, Wijtenburg SA, Chen H, Chiappelli JJ, Kochunov P, Hong LE, *et al.* Anterior cingulate glutamate and GABA associations on functional connectivity in schizophrenia. Schizophr Bull 2018. https://doi.org/10.1093/schbul/sby075.
52. Setiawan E, Wilson AA, Mizrahi R, Rusjan PM, Miler L, Rajkowska G, *et al.* Role of translocator protein density, a marker of neuroinflammation, in the brain during major depressive episodes. JAMA Psychiatry 2015, 72: 268–275.